The Plant Cell, Vol. 21: 1733–1746, June 2009, www.plantcell.org © 2009 American Society of Plant Biologists

Establishment of the Winter-Annual Growth Habit via *FRIGIDA*-Mediated Histone Methylation at *FLOWERING LOCUS C* in *Arabidopsis* [C][W]

Danhua Jiang,[a,b] Xiaofeng Gu,[a,b] and Yuehui He[a,b,1]

[a] Department of Biological Sciences, National University of Singapore, Singapore 117543, Republic of Singapore
[b] Temasek Life Sciences Laboratory, Singapore 117604, Republic of Singapore

In *Arabidopsis thaliana*, flowering-time variation exists among accessions, and the winter-annual (late-flowering without vernalization) versus rapid-cycling (early flowering) growth habit is typically determined by allelic variation at *FRIGIDA* (*FRI*) and *FLOWERING LOCUS C* (*FLC*). *FRI* upregulates the expression of *FLC*, a central floral repressor, to levels that inhibit flowering, resulting in the winter-annual habit. Here, we show that *FRI* promotes histone H3 lysine-4 trimethylation (H3K4me3) in *FLC* to upregulate its expression. We identified an *Arabidopsis* homolog of the human WDR5, namely, WDR5a, which is a conserved core component of the human H3K4 methyltransferase complexes called COMPASS-like. We found that recombinant WDR5a binds H3K4-methylated peptides and that WDR5a also directly interacts with an H3K4 methyltransferase, *ARABIDOPSIS* TRITHORAX1. *FRI* mediates WDR5a enrichment at the *FLC* locus, leading to increased H3K4me3 and *FLC* upregulation. WDR5a enrichment is not required for elevated H3K4me3 in *FLC* upon loss of function of an *FLC* repressor, suggesting that two distinct mechanisms underlie elevated H3K4me3 in *FLC*. Our findings suggest that *FRI* is involved in the enrichment of a WDR5a-containing COMPASS-like complex at *FLC* chromatin that methylates H3K4, leading to *FLC* upregulation and thus the establishment of the winter-annual growth habit.

INTRODUCTION

The timing of the developmental transition from a vegetative to a reproductive phase (i.e., flowering) is crucial to reproductive success in angiosperms. In a given environment, a plant can respond to environmental signals and integrate the responses with its developmental state to flower at a right time. In *Arabidopsis thaliana*, naturally occurring flowering-time variation exists among wild accessions, and *FRIGIDA* (*FRI*) is a major determinant of natural variation in flowering time (Johanson et al., 2000). The winter-annual (late-flowering without vernalization) versus rapid-cycling (early flowering) growth habit is often determined by allelic variation at *FRI* and *FLOWERING LOCUS C* (*FLC*) (Johanson et al., 2000; Gazzani et al., 2003; Michaels et al., 2003). FRI is a plant-specific protein with coiled-coil domains (Johanson et al., 2000), and FLC is a MADS box transcription factor that quantitatively inhibits the floral transition in *Arabidopsis* (Michaels and Amasino, 1999; Sheldon et al., 1999). Winter annuals typically have dominant alleles of *FRI* and *FLC*, whereas rapid-cycling accessions have either a nonfunctional *fri* allele or a weak *flc* allele (Johanson et al., 2000; Gazzani et al., 2003; Werner et al., 2005). The role of *FRI* is to upregulate *FLC* expression to levels that inhibit flowering, resulting in the winter-annual growth habit (Johanson et al., 2000).

FLC plays a central role in flowering-time regulation in *Arabidopsis*. In rapid-cycling accessions that lack *FRI*, autonomous pathway (AP) genes, such as *FCA*, *FPA*, *FVE*, *FY*, *LUMINIDEPENDENS*, and *FLOWERING LOCUS D* (*FLD*), constitutively repress *FLC* expression to promote flowering (Baurle and Dean, 2006). The AP gene-mediated repression can be overcome by a functional *FRI*, and introgression of *FRI* into a rapid-cycling accession, such as Columbia (Col), converts it into a winter-annual-like line (Lee et al., 1994). In winter annuals, vernalization (a prolonged cold exposure) overrides *FRI* function to repress *FLC* expression, leading to acceleration of flowering after the plants return to warm growth conditions (Michaels and Amasino, 1999; Sheldon et al., 1999).

A number of genes required for *FLC* expression (or upregulation) have been identified, and these genes can be largely classified into two groups based on their effects on *FLC* expression. One group consists of general transcriptional regulators that are required for *FLC* expression in both AP mutants and *FRI*-containing lines. For instance, mutations in *EARLY FLOWERING7* (*ELF7*) (He et al., 2004), *VERNALIZATION INDEPENDENCE5* (Oh et al., 2004), *PHOTOPERIOD-INDEPENDENT EARLY FLOWERING1* (*PIE1*) (Noh and Amasino, 2003), and *EARLY FLOWERING IN SHORT DAYS* (also known as *SDG8*) (Kim et al., 2005; Zhao et al., 2005) suppress *FLC* expression and cause early flowering. In addition to *FLC*, these genes also regulate other loci; thus, mutations in these genes give rise to pleiotropic phenotypes.

[1] Address correspondence to dbshy@nus.edu.sg.
The author responsible for distribution of materials integral to the findings presented in this article in accordance with the policy described in the Instructions for Authors (www.plantcell.org) is: Yuehui He (dbshy@nus.edu.sg).
[C]Some figures in this article are displayed in color online but in black and white in the print edition.
[W]Online version contains Web-only data.
www.plantcell.org/cgi/doi/10.1105/tpc.109.067967

The other group of genes appears to be required specifically for *FRI*-mediated *FLC* upregulation, including *FRI-LIKE1* (*FRL1*), *FRIGIDA-ESSENTIAL1* (*FES1*), and *SUPPRESSOR OF FRIGIDA4* (*SUF4*); mutations in these genes strongly suppress *FRI*-mediated *FLC* upregulation but only moderately suppress elevated *FLC* expression in AP mutants (Michaels et al., 2004; Schmitz et al., 2005; Kim et al., 2006; Kim and Michaels, 2006). SUF4 directly interacts with the *FLC* locus, can also interact with FRI in vitro, and may be involved in the recruitment of FRI to the *FLC* locus (Kim et al., 2006). However, it remains unclear how *FRI* activates *FLC* expression.

Recent studies have shown that chromatin modification plays an important role in modulating *FLC* expression. For instance, *FLC* expression requires deposition of the histone variant H2A.Z in *FLC* chromatin by a PIE1-containing complex whose known components include ACTIN-RELATED PROTEIN6 (also known as SUF3 and ESD1) and SERRATED LEAVES AND EARLY FLOWERING (also known as SWC6) (Choi et al., 2005, 2007; Deal et al., 2005, 2007; Martin-Trillo et al., 2006; March-Diaz et al., 2007). The AP genes *FLD*, *FCA*, *FPA*, and *FVE* are involved in repressive histone modifications in *FLC* and repress its expression. FLD, a plant homolog of the human Lysine-Specific Demethylase1 (LSD1) that has been found in histone deacetylase (HDAC) corepressor complexes (Shi et al., 2004; Lee et al., 2006), is involved in H3K4 demethylation and histone deacetylation in *FLC* (He et al., 2003; Jiang et al., 2007; Liu et al., 2007). Both *FCA* and *FPA*, encoding putative RNA-Recognition Motif-type RNA binding proteins, largely act through *FLD* to repress *FLC* expression (Liu et al., 2007; Baurle and Dean, 2008). FVE, a retinoblastoma-associated protein, is partly involved in histone deacetylation of *FLC* chromatin (Ausin et al., 2004). The Polycomb-repressive complex 2 subunit CURLEY LEAF (Schubert et al., 2006) directly interacts with *FLC* chromatin and mediates deposition of repressive H3 Lys-27 trimethylation in *FLC* to repress its expression (Jiang et al., 2008). In addition, histone H4 dimethylation at Arg 3 (H4R3) in *FLC* by Type I and Type II Arg methyltransferases is also associated with *FLC* repression (Niu et al., 2007; Pei et al., 2007; Wang et al., 2007). Recent studies also reveal that vernalization leads to repressive histone modifications in *FLC*, such as increased di- and trimethylation of histone H3 at Lys-9 and at Lys-27 and H4R3 dimethylation, to repress *FLC* expression (reviewed in Sung and Amasino, 2005; Baurle and Dean, 2006; He, 2009).

Histone H3K4 methylation plays an important role in regulating transcription in eukaryotes and is dynamically regulated by H3K4 methyltransferases and demethylases. The ε-amino group of H3K4 residues can be mono-, di-, and trimethylated (Dou et al., 2006; Shilatifard, 2008). H3 lysine-4 trimethylation (H3K4me3) is closely coupled with active gene expression, and the trimethyl H3K4 mark can be recognized by the evolutionarily conserved ATP-dependent chromatin remodeling machines, such as CHD1 and NURF in human, which remodel target gene chromatin leading to transcriptional activation (reviewed in Ruthenburg et al., 2007). In the well-studied *Saccharomyces cerevisiae*, H3K4 methylation is catalyzed by COMPASS (for Complex Proteins Associated with Set1), which contains an H3K4 methyltransferase known as Set1 (Miller et al., 2001). COMPASS-like complexes have been identified in human, including the hSET1

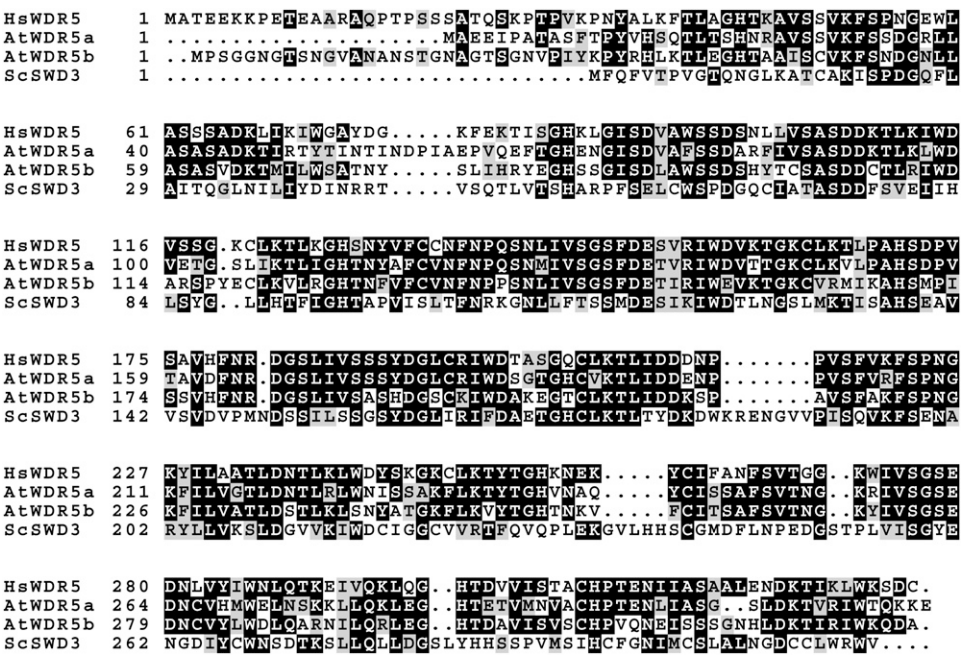

Figure 1. Amino Acid Sequence Alignment of *Arabidopsis* WDR5a (At WDR5a) and WDR5b (At WDR5b) with *S. cerevisiae* SWD3 (Sc SWD3) and *Homo sapiens* WDR5 (Hs WDR5).

Numbers refer to amino acid residues. Identical residues are shaded black, and similar residues are shaded gray.

complex and the MLL1 complex, and are capable of catalyzing H3K4 methylation and activating target gene expression (Shilatifard, 2008). All these complexes contain four evolutionarily conserved core components, namely, a relative of the yeast Set1 and three structural components, including Ash2, RbBP5, and WDR5 (Shilatifard, 2008), and an in vitro reconstituted core complex composed of these four components has H3K4-specific methyltransferase activity (Dou et al., 2006).

It has been shown that levels of H3K4me3 are increased in actively transcribed *FLC* chromatin (He et al., 2004; Pien et al., 2008). An ELF7-containing complex known as PAF1c is required for *FLC* upregulation and for the associated H3K4me3 increase in *FLC* in the *FRI* background or AP mutants (He et al., 2004; Oh et al., 2004). Furthermore, ATX1, an H3K4 methyltransferase and a homolog of the *Drosophila melanogaster* TRITHORAX and the yeast Set1 (Alvarez-Venegas et al., 2003), is also required for H3K4me3 in *FLC*, and the *atx1* mutation moderately suppresses *FLC* expression in the *FRI* background (Pien et al., 2008). In addition, *ATX2* (for *ARABIDOPSIS TRITHORAX2*), a homolog of *ATX1*, is also involved in *FLC* regulation because the *atx1 atx2* double mutation strongly suppresses *FLC* expression in the *FRI* background (Pien et al., 2008).

Although increased H3K4me3 has been shown to be associated with *FLC* chromatin in the *FRI* background, this increase is also associated with elevated *FLC* expression in AP mutants (He et al., 2004; Kim et al., 2005). Hence, the role of *FRI* in the H3K4 methylation of *FLC* chromatin is yet to be determined. In addition, little is known on how H3K4me3 is deposited at *FLC* and other loci. Furthermore, although recent studies have shown that the AP genes, such as *FLD* and *FVE*, are involved in H3K4 demethylation and deacetylation of *FLC* chromatin, it is essentially unknown how *FRI* overcomes these repressive modifications to upregulate *FLC* expression.

Here, we show that WDR5a, a homolog of a structural component of the human COMPASS-like complexes, binds histone H3 tails and also interacts with the ATX1 H3K4

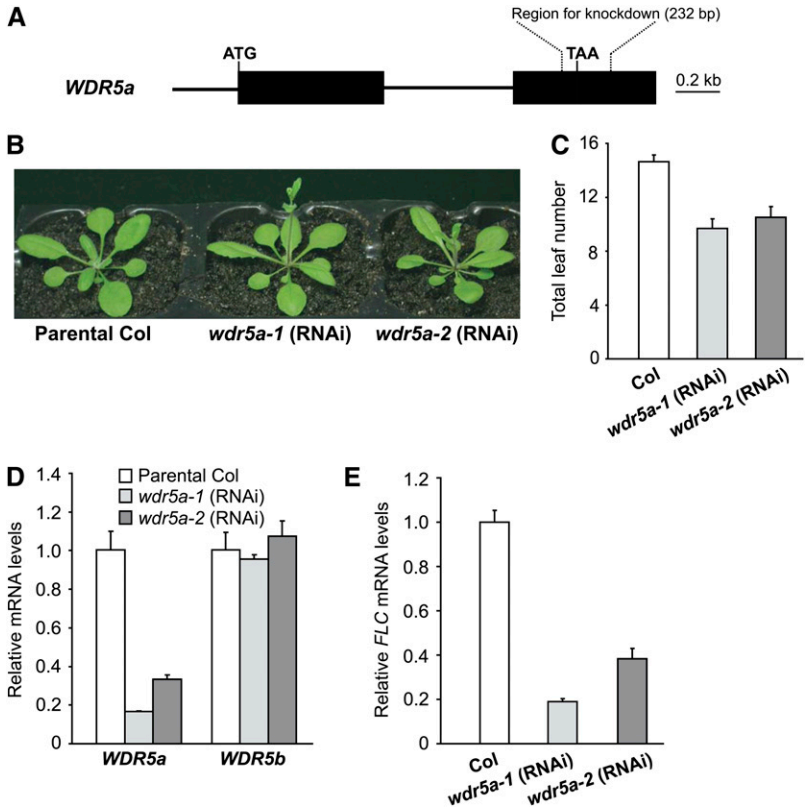

Figure 2. *WDR5a* Represses the Floral Transition in *Arabidopsis*.

(A) *WDR5a* gene structure. Exons are represented by filled boxes; the start and stop codons are marked as *ATG* and *TAA*, respectively. The 232-bp region used to knock down *WDR5a* expression is indicated by broken lines.

(B) *wdr5a* (RNAi) lines grown in long days. Col is the parental accession used in the RNAi-mediated *WDR5a* suppression.

(C) Flowering times of *wdr5a* (RNAi) lines grown in long days. The total number of primary rosette and cauline leaves at flowering was counted, and for each line, 16 plants were scored. The values shown are means ± SD.

(D) Relative mRNA levels of *WDR5a* and *WDR5b* in seedlings of *wdr5a* (RNAi) lines quantified by real-time PCR. Relative expression to parental Col is presented, with SD for three quantitative PCR replicates (**[D]** and **[E]**).

(E) Relative *FLC* mRNA levels in seedlings of *wdr5a* (RNAi) lines quantified by real-time PCR.

[See online article for color version of this figure.]

methyltransferase. *FRI* mediates WDR5a enrichment at the *FLC* locus, resulting in an increase in H3K4me3, which leads to *FLC* upregulation to inhibit flowering. Furthermore, we found that *FRI* does not disrupt the recruitment of an *FLC* repressor, FLD, to the *FLC* locus, but may compromise FLD-mediated H3K4 demethylation to overcome the *FLC* repression mediated by the AP genes *FLD*, *FCA*, and *FPA*.

RESULTS

WDR5a, an *Arabidopsis* Homolog of the Human WDR5, Represses the Floral Transition

In an effort to identify the *Arabidopsis* homologs of core components of the human COMPASS-like complexes, we found that there are two *Arabidopsis* homologs of the human *WDR5*, namely, At *WDR5a* and At *WDR5b* (Figure 1). The amino acid sequence identity between WDR5a and the human WDR5 over the entire WDR5a is 63%, and the identity between WDR5b and the human WDR5 over the entire WDR5b is 58%.

We sought to address biological functions of these two genes. First, we identified a loss-of-function mutant of *WDR5b* with a T-DNA insertion in its coding region; however, no obvious phenotypes were observed in *wdr5b* mutants (see Supplemental Figure 1 online). As no *wdr5a* mutants were identified, a double-stranded RNA interference (RNAi) approach using a *WDR5a*-specific fragment with no homology to *WDR5b* (Figure 2A), was employed to specifically knock down *WDR5a* expression. Two independent homozygous transgenic lines with a single *T-DNA* locus, *wdr5a-1* (RNAi) and *wdr5a-2* (RNAi), were created. These lines grown in long days developed normally except that they flowered earlier than the parental Col (Figures 2B and 2C). We further quantified transcript levels of *WDR5a* and *WDR5b* in

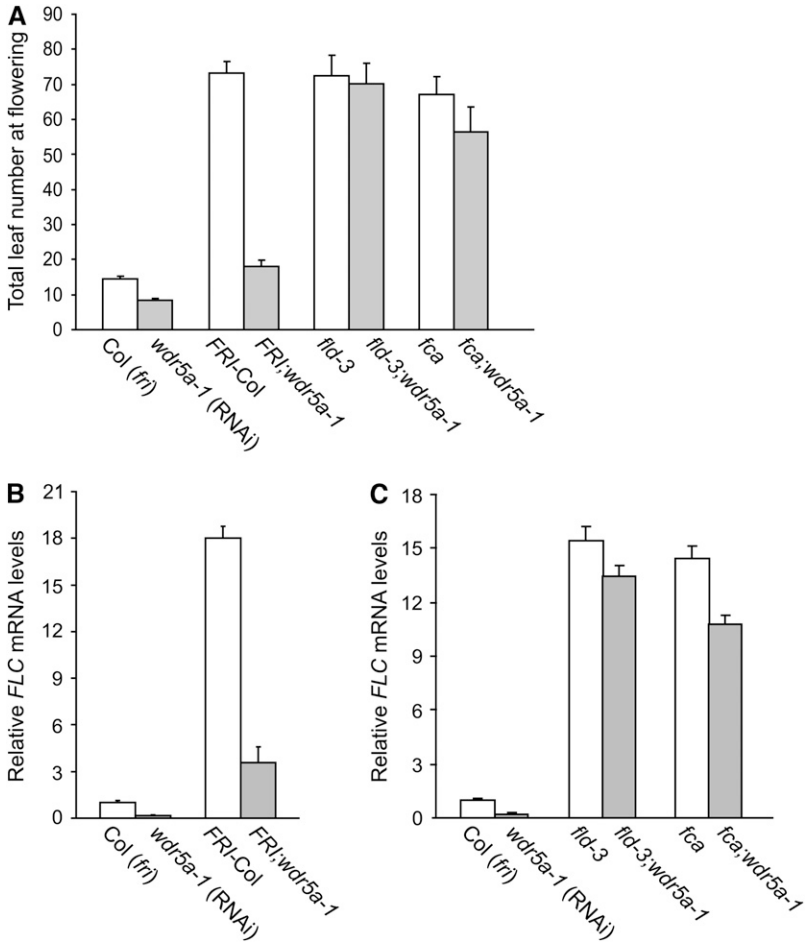

Figure 3. Effect of *WDR5a* Knockdown on *FLC*-Dependent Late Flowering.

(A) Flowering times of the indicated genotypes grown in long days. The total number of primary rosette and cauline leaves at flowering was scored, and 10 to 15 plants were counted for each line. The values shown are means ± SD.

(B) Relative *FLC* mRNA levels in seedlings of *FRI*-Col and *FRI;wdr5a-1* quantified by real-time PCR. Relative expression to Col is presented, with SD for three quantitative PCR replicates (**[B]** and **[C]**).

(C) Relative *FLC* mRNA levels in seedlings of *fld*, *fld;wdr5a-1*, *fca*, and *fca;wdr5a-1* quantified by real-time PCR.

these two lines and found that *WDR5a* expression was greatly reduced, whereas levels of *WDR5b* transcripts remained unchanged in both lines compared with Col (Figure 2D), indicating that the RNAi specifically knocks down only *WDR5a* expression. In addition, we characterized another seven independent *wdr5a* (RNAi) lines and found that all of them flowered earlier than Col (see Supplemental Table 1 online). Together, these data show that *WDR5a* represses the floral transition.

WDR5a Promotes the Expression of *FLC* and an *FLC* Homolog

FLC is a central floral repressor in *Arabidopsis*. We examined whether *WDR5a* promotes *FLC* expression to repress flowering (note that *FLC* is expressed at a low level in Col, a rapid-cycling accession) and found that *FLC* transcript levels in *wdr5a* (RNAi) lines were strongly reduced compared with Col (Figure 2E). Hence, *WDR5a* indeed upregulates *FLC* expression to delay flowering. Recent studies have shown that *FLC* homologs, including *FLOWERING LOCUS M* (*FLM*) (Scortecci et al., 2001), *MADS BOX AFFECTING FLOWERING2* (*MAF2*), and *MAF4* (Ratcliffe et al., 2003; Gu et al., 2009), moderately repress *Arabidopsis* flowering. We examined the expression of these three genes in *wdr5a-1* and *-2* (RNAi) lines and found that *MAF4* transcript levels were reduced, whereas *FLM* and *MAF2* were expressed in both lines at levels similar to those in Col (see Supplemental Figure 2 online). Thus, *WDR5a* upregulates the expression of the floral repressors *FLC* and *MAF4*. Interestingly, these two genes are still expressed at very low levels in both RNAi lines, which most likely is due to low residual levels of *WDR5a*.

As described earlier, recent studies have identified a number of genes required for *FLC* expression. We examined the expression of a few of these *FLC* regulators in *wdr5a* (RNAi) lines, including *ATX1*, *PIE1*, *ELF7*, *FRL1*, *FES1*, and *SUF4*. None of these genes was affected by *WDR5a* knockdown (see Supplemental Figure 3A online), indicating that *WDR5a* may directly promote *FLC* expression.

WDR5a Knockdown Specifically Suppresses *FRI*-Mediated *FLC* Upregulation but Not *FLC* Activation upon Loss of FLD Activity

FLC is upregulated by *FRI* and repressed by the AP genes; thus, either the presence of a functional *FRI* or a mutation in an AP gene causes delayed flowering due to elevated *FLC* expression. To evaluate the genetic interaction of *FRI* with *WDR5a* suppression, a functional *FRI* from *FRI*-Col (Lee et al., 1994) was introduced into *wdr5a-1* and *-2* (RNAi) lines. The late-flowering phenotypes conferred by *FRI* were strongly suppressed by *WDR5a* knockdown (Figure 3A; see Supplemental Figure 4 online). To evaluate the effect of *WDR5a* knockdown on *FLC* expression in the *fld* mutant, *fld* was introduced into the *wdr5a* (RNAi) lines. Interestingly, the late-flowering phenotypes of *fld* were not suppressed by *WDR5a* knockdown (Figure 3A; see Supplemental Figures 3B and 4 online). Recently, it has been shown that another AP gene *FCA* mainly acts through *FLD* to repress *FLC* expression (Liu et al., 2007). We introduced *fca* into the *wdr5a-1* line and found that the late-flowering phenotypes of *fca* mutants were only slightly suppressed by *WDR5a* knockdown (Figure 3A).

Consistent with the flowering phenotypes, elevated *FLC* expression in *fld* mutants was only slightly reduced, whereas the transcript levels of *FLC* in the *FRI* background were greatly reduced by *WDR5a* knockdown (Figures 3B and 3C). In addition, *FLC* expression in *fca* mutants was slightly suppressed by *WDR5a* knockdown (Figure 3C). To rule out the possibility of that *WDR5a* knockdown might suppress *FRI* expression, we examined *FRI* expression in *FRI*;*wdr5a-1* and found that it was

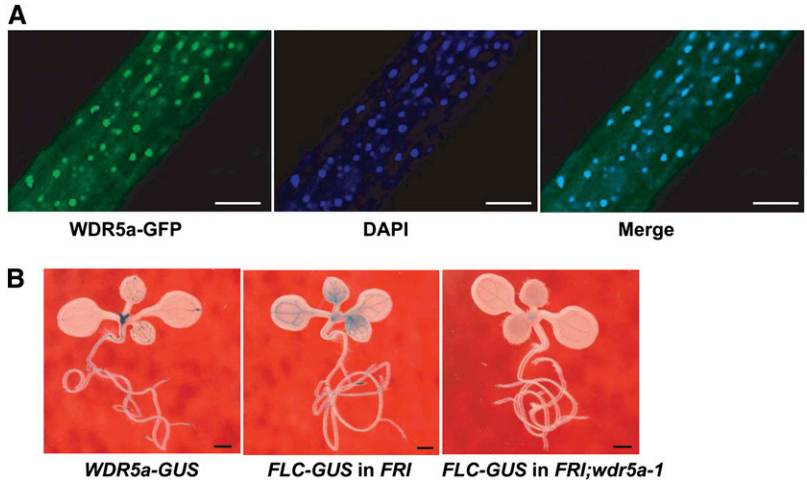

Figure 4. Cellular Localization of WDR5a and the Expression Pattern of *WDR5a*.

(A) Nuclear localization of the WDR5a-GFP fusion protein in roots of transgenic *Arabidopsis* seedlings. The blue 4',6-diamidino-2-phenylindole (DAPI) staining indicates nuclei. WDR5a-GFP and DAPI fluorescence was imaged using a laser scanning confocal microscope. Bars = 50 μm.

(B) Spatial expression patterns of the *GUS* reporter gene translationally fused to *FLC* or *WDR5a* in seedlings. The lines containing *FLC-GUS* carry a null *flc* allele. Bars = 1.0 mm.

not affected by *WDR5a* knockdown (see Supplemental Figure 3C online). Together, these data show that *WDR5a* knockdown specifically suppresses *FRI*-mediated *FLC* upregulation, but not elevated *FLC* expression in *fld* or *fca* mutants. Thus, *WDR5a* is required for *FLC* upregulation by *FRI*.

WDR5a Is Localized in the Nucleus and Preferentially Expressed in Shoot and Root Apical Regions and Vasculature

WDR5a, like the human WDR5, may act to activate target-gene expression. Consistent with its role as a transcriptional activator, the WDR5a fusion protein with green fluorescent protein (GFP) was specifically localized to the nucleus (Figure 4A). To examine the spatial expression pattern of *WDR5a*, we fused the 5′ promoter plus part of the coding region of *WDR5a* with the reporter gene *GUS* (for *β-GLUCURONIDASE*). *WDR5a* was preferentially expressed in shoot and root apical regions in seedlings, which are enriched with dividing cells, and was also expressed in vasculature (Figure 4B). This pattern is nearly identical to that of *FLC-GUS* (He et al., 2003) in the *FRI* background (Figure 4B). *WDR5a* knockdown nearly eliminated *FLC-GUS* expression in shoot apical regions and leaf vasculature in the *FRI* background (Figure 4B), consistent with the notion that *WDR5a* functions as an activator that mediates *FLC* upregulation by *FRI*.

Recombinant WDR5a Binds K4-Methylated Histone H3 Peptides

The human WDR5 recognizes and binds to the histone H3 N-terminal tail (Wysocka et al., 2005; Ruthenburg et al., 2006) and presents the H3K4 side chain for processive methylation: from unmodified K4 to mono- to di- to trimethylated form as *WDR5* knockdown causes a strong reduction in mono-, di-, and trimethyl H3K4 in human cells (Wysocka et al., 2005; Dou et al., 2006; Ruthenburg et al., 2006). It was of interest to determine whether WDR5a may directly interact with the K4-methylated H3 tails. First, glutathione *S*-transferase (GST)-tagged WDR5a was expressed in *Escherichia coli* and purified by affinity purification (Figure 5A). Next, we performed H3 peptide pull down assays using GST-WDR5a. Like the human WDR5 (Wysocka et al., 2005), the WDR5a fusion protein was enriched in the K4-mono-, di-, or trimethylated peptide pulldown with a stronger association with the K4-dimethylated H3 peptides (Figure 5B). Thus, WDR5a can recognize and bind K4-methylated H3 tails.

FRI Mediates WDR5a Enrichment at the *FLC* Locus

To investigate whether WDR5a bound to *FLC* chromatin, we performed chromatin immunoprecipitation (ChIP) using the human anti-WDR5 antibody, which recognizes both WDR5a and WDR5b (see Supplemental Figure 5 online). Previously, it has been shown that in actively transcribed *FLC* chromatin, levels of H3K4me3 increase in the region around the transcription start site (TSS) (*FLC-P*; as shown in Figure 6A) but not in the 3′ region of Intron I of *FLC* (*FLC-I*) or the middle of *FLC* (*FLC-M*) (He et al., 2004; Saleh et al., 2008a). We first quantified amounts of the immunoprecipitated *FLC* fragments from Col and *wdr5a-1* (RNAi)

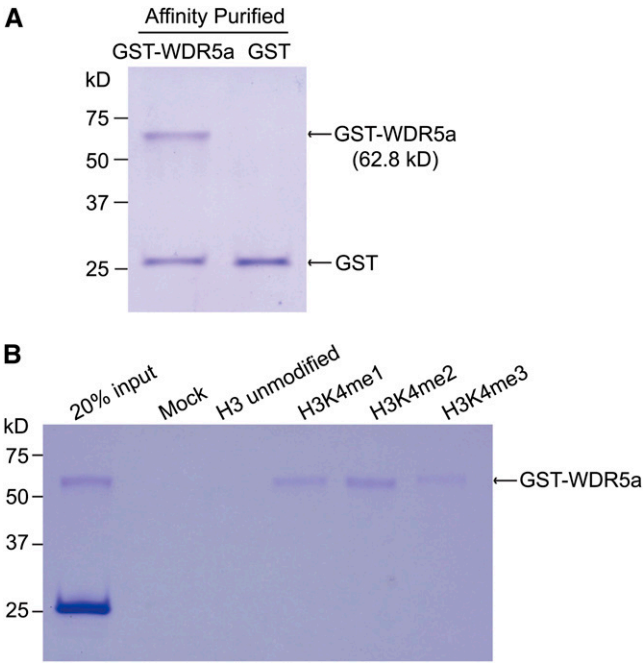

Figure 5. Histone H3 Peptide Pull-Down Assays Using a Recombinant WDR5a.

(A) Affinity-purified GST and GST-WDR5a fusion protein from *E. coli*. Proteins were analyzed by SDS-PAGE and Coomassie blue staining. The lower band in the left lane is a degradation product of GST-WDR5a. Molecular mass markers are indicated on the left.

(B) Peptide pull-down assays with GST-WDR5a and H3 peptides. A mixture of ~10-fold excess of GST with GST-WDR5a was incubated with 5.0 μg of each peptide. Proteins bound to the peptide resins were eluted and analyzed by SDS-PAGE and Coomassie blue staining. The mock is a control without any peptides.

seedlings and found that *WDR5a* knockdown led to a reduction in *WDR5a* binding to the *FLC-P* region, whereas the amounts of *FLC-I* and *FLC-M* fragments in *wdr5a-1* were similar to those in Col (see Supplemental Figure 6 online). These data suggest that WDR5a directly interacts with the *FLC* locus.

Second, we investigated whether a functional *FRI* would mediate WDR5a enrichment at *FLC* using ChIP. Indeed, we found that WDR5a was enriched in the region around TSS (*FLC-P*) but not in *FLC-I* or *FLC-M* in the presence of *FRI* (Figure 6B). Furthermore, *WDR5a* knockdown eliminates the WDR5a enrichment at *FLC-P* (Figure 6B). Together, these data show that *FRI* mediates WDR5a enrichment at the *FLC-P* region, consistent with the H3K4me3 enrichment in this region in the presence of *FRI* (He et al., 2004) (also see Figure 6D).

Third, we examined whether in *fld* mutants WDR5a binding to *FLC* chromatin was also increased but found that WDR5a was not enriched in *FLC-P*, *FLC-I*, or *FLC-M* in *fld* relative to wild-type Col (Figure 6C). Hence, WDR5a enrichment is not associated with elevated *FLC* expression upon loss of FLD activity. Interestingly, *WDR5a* knockdown led to a moderate reduction in WDR5a binding to *FLC-P* in *fld;wdr5a-1* relative to *fld* and Col

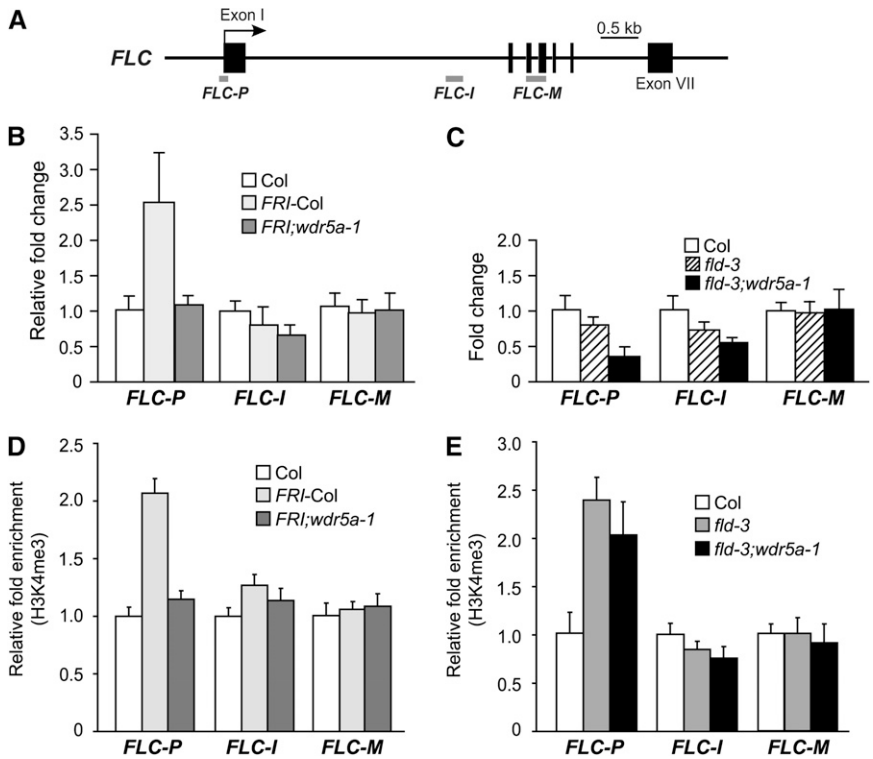

Figure 6. Role of WDR5a in *FLC* activation.

(A) Schematic structure of genomic *FLC* and the regions examined by ChIP. The arrow indicates the transcription start site; filled boxes represent exons.

(B) WDR5a enrichment at the *FLC* locus in presence of *FRI*. The amounts of *FLC* fragments immunoprecipitated from seedlings were quantified by real-time PCR and subsequently normalized to an internal control (*TUBLIN2* [*TUB2*]). The fold enrichments of *FRI*-Col and *FRI;wdr5a-1* over Col are shown. Data in the graphs are average values from two ChIP experiments (each quantified in triplicate), and error bars represent SD (**[B]** to **[E]**).

(C) Loss of *FLD* function does not cause WDR5a enrichment at the *FLC* locus.

(D) Relative levels of trimethyl H3K4 in *FLC* chromatin in Col, *FRI*-Col, and *FRI;wdr5a-1* seedlings determined by real-time quantitative PCR. The amounts of DNA fragments after ChIP were quantified and subsequently normalized to an internal control (*TUB2*). The fold changes of *FRI*-Col and *FRI; wdr5a-1* over Col at the indicated regions are shown.

(E) Relative levels of trimethyl H3K4 in *FLC* chromatin in Col, *fld-3*, and *fld-3;wdr5a-1* seedlings. The fold changes of *fld-3* and *fld-3;wdr5a-1* over Col at the indicated regions are shown.

(Figure 6C), which may contribute to a slight reduction in *FLC* expression in *fld* mutants as shown in Figure 3C.

WDR5a Enrichment at *FLC* Is Required Specifically for Elevated H3K4me3 in the Presence of *FRI*

To investigate the effect of *WDR5a* knockdown on the H3K4me3 state in *FLC* in the *FRI* background, we performed ChIP using anti-H3K4me3. Consistent with the previous findings (He et al., 2004), H3K4me3 was enriched in the region around TSS in the *FRI* background. Furthermore, we found that *WDR5a* knockdown eliminated this H3K4me3 enrichment in *FLC-P* (Figure 6D); hence, this enrichment mediated by a functional *FRI* is WDR5a dependent.

We further examined the H3K4me3 state of *FLC* chromatin in *fld* mutants upon *WDR5a* knockdown. Consistent with our previous findings (He et al., 2004; Jiang et al., 2007), H3K4me3 was enriched in the *FLC-P* region but not in *FLC-I* in *fld* relative to Col (Figure 6E). Recent studies show that dimethylated H3K4 is enriched in the middle of *FLC* (*FLC-M*) upon loss of FLD activity (Liu et al., 2007). Interestingly, the levels of H3K4me3 in *FLC-M* were not increased in *fld* relative to Col (Figure 6E).

Next, we compared the levels of H3K4me3 in *FLC-P* in *fld* and *fld;wdr5a-1* seedlings. In contrast with the strong reduction in H3K4me3 in the *FRI* background upon *WDR5* knockdown (Figure 6D), the level of H3K4me3 in *FLC-P* in *fld;wdr5a-1* was close to that in *fld* (Figure 6E); hence, *WDR5a* suppression has little effect on H3K4me3 in *FLC* chromatin upon loss of FLD activity. Together, these data show that WDR5a enrichment at *FLC* chromatin is required specifically for the H3K4me3 increase in the presence of *FRI*.

WDR5a Interacts with the ATX1 Histone H3K4 Methyltransferase

As noted above, WDR5a enrichment at *FLC* is required for *FRI*-mediated increase of H3K4me3 in *FLC* chromatin. WDR5a is

expected to act in the context of an H3K4 methyltransferase complex to promote *FLC* expression. Recent studies show that ATX1, an H3K4 methyltransferase (Alvarez-Venegas et al., 2003), is required for H3K4me3 in *FLC* (Pien et al., 2008). We sought to address whether WDR5a and ATX1 act as part of a complex that catalyzes H3K4me3. First, yeast two-hybrid assays were performed using the full-length WDR5a and ATX1 proteins; we found that these two proteins interacted strongly in yeast (Figure 7A). Next, we performed GST-ATX1 pull-down experiments using protein extracts from *E. coli* expressing GST-ATX1 or recombinant WDR5a (see Supplemental Figure 7 online) and found that GST-ATX1, but not GST, could effectively bind WDR5a (Figure 7B). Together, these data suggest that WDR5a and ATX1 may act in a complex to mediate H3K4 methylation.

Effect of *FRI* and Loss of *FLD* Function on *FLC* Upregulation

FRI can override *FLD*-mediated *FLC* repression to upregulate *FLC* expression in winter annuals. We sought to address how *FRI* might interfere with *FLD* function. We first investigated the

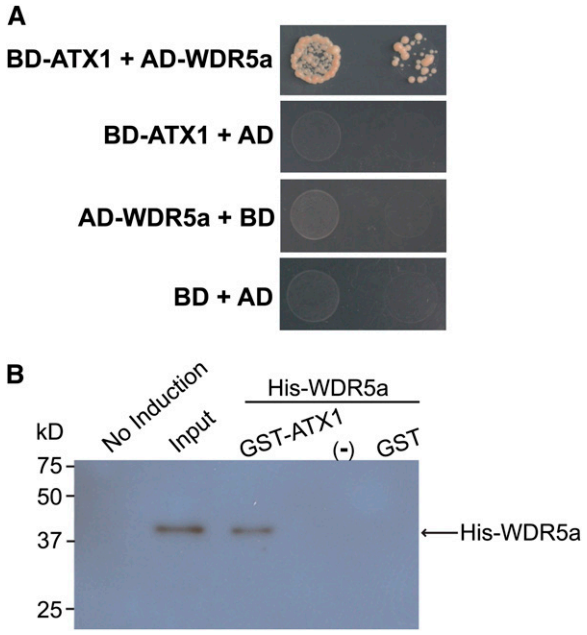

Figure 7. WDR5a Interacts with the ATX1 Histone H3K4 Methyltransferase.

(A) Interaction of WDR5a with ATX1 in yeast. Full-length WDR5a and ATX1 proteins were fused to GAL4 activation (AD) and DNA binding domains (BD), respectively. Yeast strains harboring these fusion constructs and/or empty vectors, as indicated, were grown on a selective medium lacking histidine and adenine.

(B) GST-ATX1 pull-down assays. An equal amount of the bacteria extract containing GST or GST-ATX1, or noninduced *E. coli* extract indicated as −, was incubated with the extract containing His-WDR5a. Proteins were recovered using glutathione-linked resins and analyzed by immunoblotting with anti-WDR5. Input corresponds to ~3% of the His-WDR5a extract used in the pull-down assays.

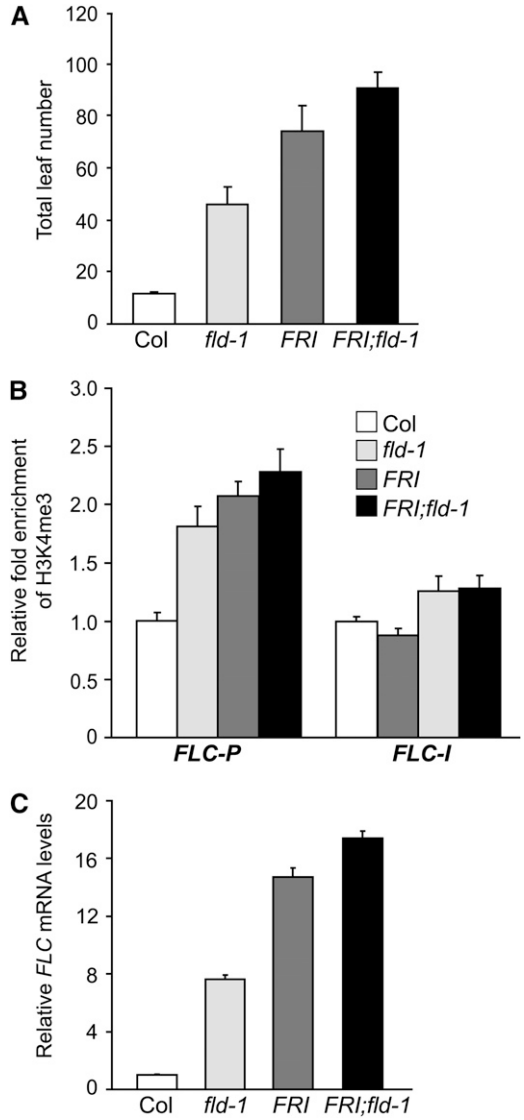

Figure 8. Effect of *FRI* and Loss of FLD Activity on H3K4me3 in *FLC* Chromatin and *FLC* Upregulation.

(A) Flowering times of Col, *fld-1* (a weak allele), *FRI*-Col, and *FRI;fld-1* grown in long days. The total number of primary rosette and cauline leaves at flowering was scored, and 13 to 15 plants for each line were counted. The values shown are means ± SD.

(B) Relative levels of trimethyl H3K4 in *FLC* chromatin in Col, *fld-1*, *FRI*-Col, and *FRI;fld-1* seedlings. The fold changes of the indicated genotypes over Col at the indicated regions are shown (Col and *FRI*-Col as described in Figure 6D). Data in the graphs are average values from two ChIP experiments (each quantified in triplicate), and error bars represent SD. The examined regions are as illustrated in Figure 6A.

(C) Relative *FLC* mRNA levels in seedlings of Col, *fld-1*, *FRI*-Col, and *FRI;fld-1* quantified by real-time PCR. Relative expression to Col is presented, with SD for three quantitative PCR replicates.

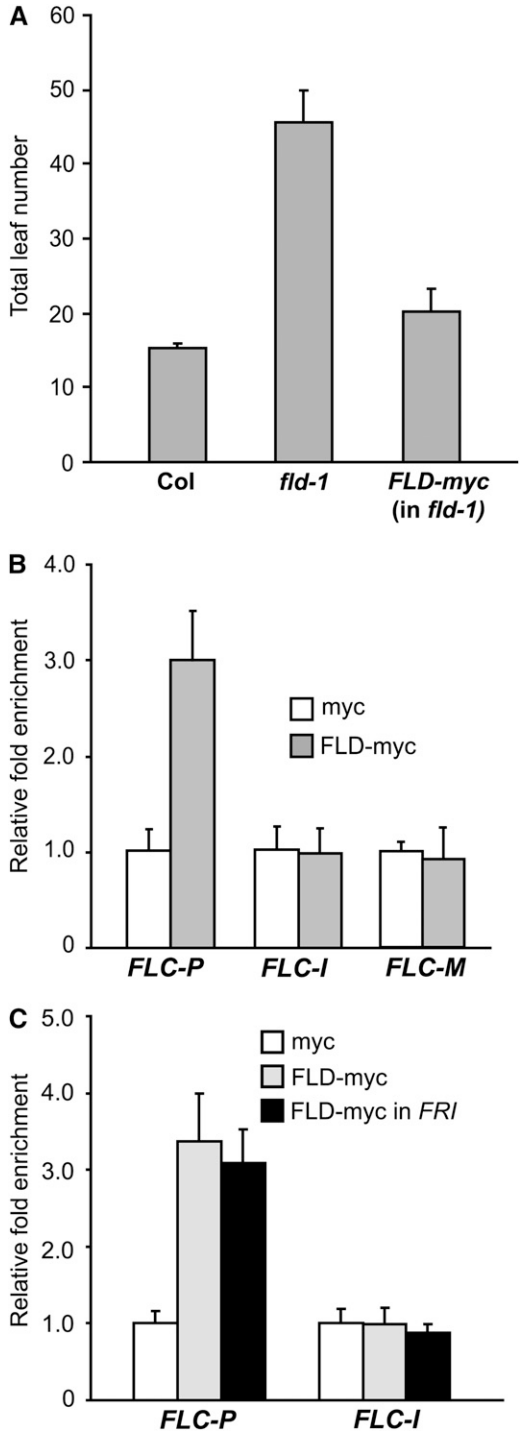

Figure 9. Recruitment of FLD to the *FLC* Locus.

(A) *FLD-myc* rescues the late-flowering phenotypes of *fld-1* mutants grown in long days. The total number of primary rosette and cauline leaves at flowering was scored, and 7 to 10 plants were counted for each line.

(B) Recruitment of FLD to the *FLC* locus. The amounts of *FLC* fragments immunoprecipitated from seedlings of an *fld-1* mutant line expressing a functional FLD-myc (labeled as FLD-myc) and a transgenic Col line expressing *35S Promoter-myc* (labeled as myc) were quantified by real-time PCR and subsequently normalized to an internal control (*TUB2*). The fold enrichments of FLD-myc over the control (myc) are shown. Data in the graphs are average values from two ChIP experiments (each quantified in triplicate), and error bars are SD (**[B]** and **[C]**). The examined regions are as illustrated in Figure 6A.

(C) Recruitment of FLD to the *FLC* locus in the presence of *FRI*. The amounts of DNA fragments immunoprecipitated from seedlings of myc, FLD-myc, and a *FRI/-;fld-1* line expressing a functional FLD-myc (labeled as FLD-myc in *FRI*) were quantified by real-time PCR and subsequently normalized to *TUB2*. The fold enrichments of the indicated genotypes over the control (myc) are shown.

genetic interaction of *FRI* with *fld*. A functional *FRI* was introduced into an *fld* mutant. *FRI;fld* flowered later than either *fld* or *FRI*-Col (Figure 8A). Furthermore, we examined the H3K4me3 state of *FLC* chromatin in *FRI*-Col, *fld*, and *FRI;fld* seedlings using ChIP. The levels of H3K4me3 in *FRI;fld* were higher than those in either *FRI*-Col or *fld* (Figure 8B). In addition, we examined *FLC* expression in these lines and found that the transcript levels of *FLC* in *FRI;fld* were higher than those in either *FRI*-Col or *fld* (Figure 8C), consistent with the H3K4me3 levels in these lines. Hence, the effect of *FRI* and loss of *FLD* function on the H3K4me3 state and *FLC* upregulation appears partially additive.

FRI Does Not Disrupt the Recruitment of FLD to *FLC* Chromatin but May Compromise *FLD* Function

Although it has been shown that *FLD* is an *FLC* repressor, it was unknown whether FLD acted directly on the *FLC* locus or indirectly. To examine the interaction of FLD with the *FLC* locus, we performed ChIP assays using a transgenic line expressing a functional myc-tagged FLD (Figure 9A). FLD was enriched in the region around TSS of *FLC* but not in the 3′ region of Intron I or the middle of *FLC* (Figure 9B). Thus, FLD interacts with *FLC* chromatin to mediate H3K4 demethylation in *FLC*.

Next, we investigated the effect of *FRI* on FLD binding to *FLC* chromatin and, surprisingly, found that in the presence of *FRI*, FLD still bound to *FLC* chromatin and that levels of FLD recruited to the *FLC* locus were similar with and without *FRI* (Figure 9C). Thus, *FRI* does not disrupt the recruitment of FLD to *FLC* chromatin. The FLD protein at *FLC* is at least partially functional because loss of FLD activity gives rise to a moderate increase of H3K4me3 in *FLC* in the *FRI* background (Figure 8B). Interestingly, FLD function appears compromised in the presences of *FRI* as indicated by the less than predicted fully additive effect of *FRI* and *fld* on H3K4me3 in *FLC*.

DISCUSSION

In this study, we show that *FRI* mediates the enrichment of WDR5a at *FLC* chromatin and that WDR5a can bind the K4-methylated H3 tails and directly interact with the ATX1 H3K4 methyltransferase. The enrichment of WDR5a causes elevated H3K4me3 in *FLC* and *FLC* upregulation. In rapid-cycling accessions that lack *FRI*, an AP component, FLD, is recruited to the *FLC* locus to mediate H3K4 demethylation, and loss of FLD

activity causes an increase in H3K4me3 that does not require WDR5a enrichment at *FLC* chromatin. *FRI* does not disrupt the recruitment of FLD to the *FLC* locus but may compromise FLD function. Our findings suggest that *FRI* is involved in the enrichment of a WDR5a-containing COMPASS-like complex at the *FLC* locus that methylates H3K4, leading to *FLC* upregulation and thus the establishment of winter-annual growth habit.

Two Distinct Mechanisms Underlie Elevated H3K4me3 in *FLC* Chromatin

Previously, it has been shown that elevated H3K4me3 in *FLC* chromatin is associated with *FLC* upregulation in the *FRI* background or AP mutants, such as *fld* and *fca*, and requires the PAF1c complex (He et al., 2004; Kim et al., 2005); however, the underlying mechanisms are unclear. The findings in this study suggest that there are two distinct mechanisms by which H3K4me3 can be elevated at the *FLC* locus. In the first mechanism, *FRI* mediates WDR5a enrichment followed by H3K4me3 enrichment at the *FLC* locus, particularly in the region around the transcription start site, part of which is required for elevated *FLC* expression because an 80-bp deletion in the 5′ untranslated region of the *FLC-P* region suppresses *FLC* expression (He et al., 2004). The H3K4me3 enrichment in the presence of *FRI* requires WDR5a. In the second mechanism, loss of FLD activity disrupts H3K4 demethylation, resulting in H3K4me3 enrichment in *FLC* chromatin. This does not require WDR5a enrichment at the *FLC* locus. Therefore, both WDR5a enrichment-dependent H3K4 methylation and disruption of H3K4 demethylation can cause elevated H3K4me3 in *FLC* chromatin.

FLD-Mediated H3K4 Demethylation in *FLC* Chromatin

FLD is a plant homolog of the human LSD1 that has been found in HDAC corepressor complexes and demethylates mono- and dimethyl H3K4 (Shi et al., 2004; Lee et al., 2006). Upon loss of FLD activity, H3K4me3, and to a lesser degree, H3K4 dimethylation in *FLC* chromatin increase (He et al., 2004; Jiang et al., 2007; Liu et al., 2007). The increase in H3K4me3 may be due to an increased availability of dimethyl H3K4 to an H3K4-methyltransferase complex (also see discussion below); on the other hand, the reduction of H3K4me3 in the presence of FLD may be attributed to a decrease in the dimethyl K4 level.

There are several lines of evidence to suggest that FLD functions as an H3K4 demethylase. First, a point mutation that changes a Pro into a Leu in the conserved FAD (for flavin adenine dinucleotide; a cofactor for catalysis) binding subdomain in the FLD protein eliminates its function (Chen et al., 2006; Liu et al., 2007). In addition, we noticed that the purified FLD protein from *E. coli*, like the purified LSD1, was light yellow, which is characteristics of FAD binding proteins (Shi et al., 2004). Second, recent studies show that LSD1 LIKE1 (LDL1), another *Arabidopsis* homolog of LSD1, specifically demethylates H3K4 and that *LDL1* mediates H3K4 demethylation in *FLC* and acts in partial redundancy with *FLD* to repress *FLC* expression (Jiang et al., 2007; Spedaletti et al., 2008). Taken together, these findings suggest that FLD and LDL1 function as H3K4 demethylases to repress *FLC* repression.

A Putative WDR5a-Containing H3K4 Methyltransferase Complex Involved in *FRI*-Mediated H3K4me3 in *FLC*

The yeast COMPASS complex and the human COMPASS-like complexes all contain four evolutionarily conserved core components (Shilatifard, 2008). Besides WDR5a and WDR5b, *Arabidopsis* also has homologs of the other three core components of the COMPASS-like complexes, including seven homologs of the yeast Set1 H3K4 methyltransferase (two of these homologs are ATX1 and ATX2) (Alvarez-Venegas et al., 2003; Springer et al., 2003), a single homolog of RbBP5, and a single homolog of Ash2 (data not shown), suggesting that COMPASS-like complexes are evolutionarily conserved in *Arabidopsis*.

Recent studies show that both *ATX1* and *ATX2* are involved in *FLC* regulation (Pien et al., 2008). ATX1, an H3K4 methyltransferase, is directly involved in H3K4me3 in *FLC* chromatin and required for *FLC* upregulation in the presence of *FRI* (Pien et al., 2008), whereas the biochemical role of ATX2 in *FLC* regulation is unclear, as its biochemical function is distinct from ATX1 (Saleh et al., 2008b). We have found that WDR5a interacts with ATX1, suggesting that these proteins may act in a complex. In addition, the spatial expression patterns of *WDR5a*, *ATX1*, and *FLC* overlap. It has been shown that like *FLC*, the *GUS* reporter

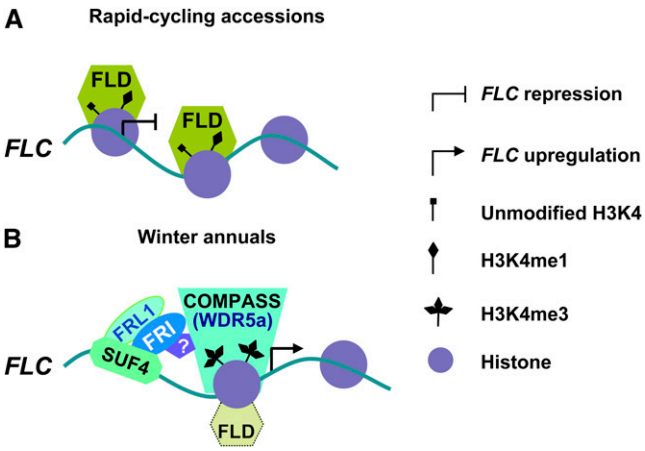

Figure 10. Model for Regulation of *FLC* Expression by *FRI* and *FLD*.

(A) In rapid-cycling accessions, *FLD* mediates repressive histone modifications to repress *FLC* expression and thus accelerate flowering. FLD (or a putative FLD-containing HDAC corepressor complex) is recruited to the *FLC* locus and mediates demethylation of mono- and dimethyl H3K4 and deacetylation of core histone tails to establish a repressive chromatin environment.

(B) *FRI* mediates WDR5a enrichment followed by elevated H3K4me3 in *FLC* to upregulate *FLC* expression resulting in the winter-annual growth habit. In winter annuals, SUF4 recognizes and binds to the *FLC* promoter and subsequently recruits FRI and FRL1 to the *FLC* locus. FRI may promote the recruitment of a WDR5a-containing COMPASS-like H3K4 methyltransferase complex to *FLC* chromatin to catalyze H3K4 methylation and may also cause a partial disruption of the function of FLD or an FLD complex, resulting in *FLC* upregulation. FRL1 and/or other cofactors may be involved in FRI-mediated enrichment of a WDR5a-containing complex at *FLC*.

[See online article for color version of this figure.]

driven by the *ATX1* promoter, can be readily detected in vasculature and shoot and root apical regions in seedlings (Saleh et al., 2008b). We have found that like *FLC*, *WDR5a* is preferentially expressed in vasculature and shoot and root apical regions in seedlings. Together, these findings suggest that ATX1 is part of a WDR5a-containing complex that is enriched at the *FLC* locus by a functional *FRI* to methylate H3K4, leading to *FLC* activation.

The human WDR5 is an essential structural component of the COMPASS-like H3K4 methyltransferase complexes. It recognizes and binds H3 tails as revealed by peptide pulldown and peptide binding assays and functions to present H3K4 for methylation by an H3K4 methyltransferase (Wysocka et al., 2005; Dou et al., 2006; Ruthenburg et al., 2006). We have found that WDR5a can bind to K4-methylated H3 peptides with a stronger association with H3K4me2. Although the recombinant WDR5a was not enriched in the K4-unmodified H3 peptide pulldown (Figure 5B), it is likely that WDR5a may recognize and bind unmodified H3K4 peptides at a low affinity. Given the close homology and functional similarity of WDR5a and the human WDR5, it is likely that WDR5a may function to present the H3K4 side chain for methylation in target loci.

H3K4 Methylation in *fld;wdr5a* (RNAi) Mutants

Levels of methylated H3K4 are dynamically regulated by H3K4 methyltransferases and demethylases. Prior to being demethylated, the K4 residues must be methylated first; hence, although disruption of H3K4 demethylation at the *FLC* locus upon loss of FLD activity causes an increase in methylated K4 residues, it is expected that at least a low level of H3K4 methylation would still be required for the increase in H3K4me3 in *fld* mutants. Interestingly, knockdown or suppression of WDR5a-dependent H3K4 methylation in *FLC* has little effect on the H3K4 trimethylation of *FLC* chromatin in *fld* mutants. One possibility is that the elevated H3K4 trimethylation upon loss of FLD activity is WDR5a independent. A second possibility is that in the event of WDR5a knockdown, the remaining WDR5a proteins (see Supplemental Figure 5 online) may act in the context of an ATX1-containing COMPASS-like complex to processively convert mono- and dimethyl H3K4 to trimethyl H3K4 in *fld* mutants. As noted above, loss of FLD activity is expected to give rise to an increase in both mono- and dimethyl H3K4, and the increased substrate availability to the H3K4 methyltransferase complex at the *FLC* locus in *fld* mutants may compensate for the reduced complex levels upon WDR5a knockdown.

FRI-Mediated WDR5a Enrichment at the *FLC* Locus

Although both *FRI* and loss of FLD activity lead to elevated H3K4me3 in *FLC*, we have found that WDR5a is enriched at the *FLC* locus only in the presence of *FRI*. As noted above, WDR5a and ATX1 may act as part of a COMPASS-like complex to methylate H3K4 in *FLC*. Now the question is how a functional *FRI* mediates the enrichment of a WDR5a-containing complex at the *FLC* locus. Recent studies show that SUF4, a zinc finger protein, directly binds the *FLC* promoter and that SUF4 also can interact with FRI and an FRI homolog, FRL1, and may be involved in the recruitment of FRI to the *FLC* locus (Kim et al., 2006; Kim and Michaels, 2006). As illustrated in Figure 10, we speculate that the FRI proteins localized in the *FLC* locus via SUF4 may promote the recruitment of a WDR5a- and ATX1-containing COMPASS-like complex to this locus, leading to elevated H3K4me3 and thus *FLC* upregulation.

As noted earlier, *FRI* can override *FLD* to upregulate *FLC* expression in winter annuals. We have found that *FRI* does not disrupt the recruitment of FLD (or FLD-containing corepressor complex) to *FLC* chromatin but may partially disrupt FLD function. Because the AP genes *FCA* and *FPA* mainly function through *FLD* to repress *FLC* expression (Liu et al., 2007; Baurle and Dean, 2008), a functional *FRI* may also disrupt the *FLC* repression mediated by these two genes. Taken together, our study suggests that *FRI* may play a dual role in the H3K4 trimethylation of *FLC* chromatin, namely, enriching an H3K4 methyltransferase complex and compromising H3K4 demethylation at *FLC*, to upregulate *FLC* expression and thus establish the winter-annual growth habit.

METHODS

Plant Materials and Growth Conditions

Arabidopsis thaliana fld-1, *fld-3* (He et al., 2003), *fca-9* (Baurle and Dean, 2008), and *FRI*-Col (Lee et al., 1994) were described previously. The *wdr5b* mutant was isolated from the Versailles transformant collection (Samson et al., 2002). Plants were grown under cool white fluorescent light in long days (16 h light /8 h night) at ~22°C.

RNA Analysis

Total RNAs from aerial parts of ~10-d-old seedlings grown in long days were extracted as described previously (Jiang et al., 2007). cDNAs were reverse transcribed from total RNAs with Moloney murine leukemia virus reverse transcriptase (Promega). Real-time quantitative PCR was performed on an ABI Prism 7900HT sequence detection system using SYBR Green PCR master mix as described previously (Jiang et al., 2007). Each sample was quantified in triplicate and normalized using *TUB2* (At_*5g62690*) as the endogenous control. Primers used for the amplification of *FLC*, *FLM*, *MAF2*, *MAF4*, *TUB2*, and *ACT2* have been described previously (Jiang et al., 2007; Gu et al., 2009), and the primers used for *WDR5a* and *WDR5b* amplification are specified in Supplemental Table 2 online.

Knockdown of *WDR5a* Expression via Double-Stranded RNAi

A 232-bp *WDR5a*-specific fragment (from +957 to +1188 of *WDR5a* cDNA; the transcription start site is set as +1) was used to create a hairpin RNA by the AGRICOLA consortium (Hilson et al., 2004); the resulting binary plasmid was introduced into *Agrobacterium tumefaciens* strain *GV3101* carrying *pMP90* and *pSOUP* helper plasmids through electroporation and subsequently was introduced into Col by the floral dip method (Clough and Bent, 1998).

Plasmid Construction

To construct the *WDR5a-GFP* plasmid, the entire coding sequence of *WDR5a* except the stop codon (1.0 kb) was inserted between the 35S promoter and *GFP* in the *pMDC85* vector (Curtis and Grossniklaus, 2003) via Gateway technology (Invitrogen); the coding sequence is in-frame with the downstream *GFP* reporter gene. To construct the *WDR5a-GUS*

plasmid, a 1.75-kb *WDR5a* genomic fragment (from −1617 to +150; A of the start codon as +1) including a 1.6-kb 5′ promoter plus a 0.15-kb genomic coding sequence was inserted into the *pBGWFS7* vector (Karimi et al., 2005) via Gateway technology; the genomic coding sequence is in-frame with the downstream *GUS* reporter gene. To construct the *FLD-myc* plasmid, a 4424-bp *FLD* (from −1900 to +2524; A of the start codon as +1) genomic fragment including a 1.9-kb 5′ promoter plus the 2.5-kb genomic coding sequence was inserted into a vector derived from *pC-TAPa* (Rubio et al., 2005) in which a stop codon has been introduced in between the coding sequences for the 9x c-myc tag and the IgG binding domain; *FLD* is in-frame with the downstream 9x *c-myc*.

Peptide Pull-Down Assay

GST-WDR5a and GST were overexpressed in *Escherichia coli* and affinity-purified using glutathione-linked resins according to the manufacturer's instructions (Sigma-Aldrich). Peptide pulldown was performed as described by Wysocka et al. (2005). Briefly, a mixture of ~10-fold excess of GST (40 μg) with ~4.0-μg GST-WDR5a (estimated) was first precleared with avidin beads (Sigma-Aldrich); subsequently, 5.0-μg H3 peptides with unmodified, mono-, di-, or trimethylated K4, conjugated with biotin (Millipore), were incubated with the avidin beads and the protein mixture; beads were washed six times and subsequently the proteins bound to the beads were eluted by boiling using a 2× SDS-PAGE loading buffer. The mock is a control in which the protein mixture was incubated with the avidin beads alone. Elutes were analyzed by SDS-PAGE and Coomassie Brilliant Blue staining.

Protein Pull-Down Assay

The pulldowns were performed as described by Calonje et al. (2008). Briefly, after isopropyl-β-D-thiogalactopyranoside induction, *E. coli* (BL21 DE3) cells expressing GST-ATX1, His-WDR5a, or GST were harvested by centrifugation, resuspended in 1.0-mL binding buffer (20 mM Tris-HCl, pH 7.5, 150 mM NaCl, 0.1% Triton X-100, 10% glycerol, 1 mM phenylmethylsulphonyl fluoride, and 1× Roche proteinase inhibitors), and sonicated. The protein extracts were centrifuged and an equal amount of the extract (300 μL for each extract) containing GST or GST-ATX1, or noninduced *E. coli* extract, was mixed with the His-WDR5a extract with rotating for 4 h at 4°C; subsequently, 40 μL of glutathione-linked resins (Sigma-Aldrich) was added into the mixture and incubated with rotating for another 2 h at 4°C. The beads were washed four times with the binding buffer. Proteins were eluted and further analyzed by immunoblotting using an antibody raised against the human WDR5 (Abcam).

ChIP and Real-Time Quantitative PCR Assay

The ChIP experiments were performed as described previously using 10-d-old seedlings (Johnson et al., 2002). Rabbit polyclonal anti-trimethyl-histone H3 (Lys 4) (Abcam), anti-WDR5 (Abcam), and anti-c-Myc (Lab Vision) were used in the immunoprecipitation experiments. Rabbit IgG (Millipore) was used as a negative control in each ChIP experiment to check the background levels of DNA fragments. The amounts of the immunoprecipitated genomic DNA were quantified by real-time PCR. Quantitative measurements of *FLC-P*, *FLC-I*, and *FLC-M* fragments were performed on an ABI Prism 7900HT sequence detection system using SYBR Green PCR master mix. Primers used to amplify *FLC-P* and *TUB2* have been described previously (Jiang et al., 2007), and primers used to amplify *FLC-I* and *FLC-M* are specified in Supplemental Table 2 online. Each of the immunoprecipitations was repeated independently once. The relative fold changes are the average of six measurements of two ChIP experiments (each quantified in triplicate), and error bars are standard deviations of the six quantitative PCR assays.

Accession Numbers

Sequence data from this article can be found in the GenBank/EMBL data libraries under accession numbers At_*3g49660* (*WDR5a*) and At_*4g02730* (*WDR5b*).

Supplemental Data

The following materials are available in the online version of this article.

Supplemental Figure 1. Analyses of a Loss-of-Function *wdr5b* Mutant.

Supplemental Figure 2. Relative mRNA Levels of *FLM*, *MAF2*, and *MAF4* in Seedlings of *wdr5a* (RNAi) Lines Quantified by Real-Time PCR.

Supplemental Figure 3. Analysis of Expression of the Indicated Genes upon *WDR5a* Knockdown.

Supplemental Figure 4. Effect of *WDR5a* Knockdown on the Late-Flowering Phenotypes of *FRI*-Col and *fld* Grown in LDs.

Supplemental Figure 5. Immunoblot Analysis of WDR5a in the Indicated Lines Using an Antibody Raised against the Human WDR5.

Supplemental Figure 6. *WDR5a* Knockdown Leads to Decreased Binding of WDR5a to *FLC* Chromatin.

Supplemental Figure 7. SDS-PAGE Analysis of Total Protein Extracts from *E. coli* Harboring *GST-ATX1*, *His-WDR5a*, or *GST* Plasmids.

Supplemental Table 1. Total Leaf Number at Flowering of *wdr5a* (RNAi) Lines Grown in Long Days.

Supplemental Table 2. Sequences of Primers Used in RT-PCR and ChIP-PCR Experiments.

ACKNOWLEDGMENTS

We thank Toshiro Ito and R. Jose Dinney for critically reading this manuscript, Wannian Yang and Jiafu Jiang for experimental assistance, and the AGRICOLA consortium for providing the double-stranded RNAi plasmid targeting *WDR5a*. This work was supported by grants from the Singapore Ministry of Education (AcRF Tier 2; T207B3105) and the National University of Singapore (AcRF Tier 1; R-154-000-294-112) and by the Temasek Life Sciences Laboratory to Y.H.

Received April 16, 2009; revised May 17, 2009; accepted June 4, 2009; published June 30, 2009.

REFERENCES

Alvarez-Venegas, R., Pien, S., Sadder, M., Witmer, X., Grossniklaus, U., and Avramova, Z. (2003). *ATX-1*, an *Arabidopsis* homolog of *TRITHORAX*, activates flower homeotic genes. Curr. Biol. **13:** 627–637.

Ausin, I., Alonso-Blanco, C., Jarillo, J.A., Ruiz-Garcia, L., and Martinez-Zapater, J.M. (2004). Regulation of flowering time by FVE, a retinoblastoma-associated protein. Nat. Genet. **36:** 162–166.

Baurle, I., and Dean, C. (2006). The timing of developmental transitions in plants. Cell **125:** 655–664.

Baurle, I., and Dean, C. (2008). Differential interactions of the autonomous pathway RRM proteins and chromatin regulators in the silencing of *Arabidopsis* targets. PLoS ONE **3:** e2733.

Calonje, M., Sanchez, R., Chen, L., and Sung, Z.R. (2008). *EMBRYONIC*

FLOWER 1 participates in polycomb group-mediated *AG* gene silencing in *Arabidopsis.* Plant Cell **20:** 277–291.

Chen, Y., Yang, Y., Wang, F., Wan, K., Yamane, K., Zhang, Y., and Lei, M. (2006). Crystal structure of human histone Lysine-Specific Demethylase 1 (LSD1). Proc. Natl. Acad. Sci. USA **103:** 13956–13961.

Choi, K., Kim, S., Kim, S.Y., Kim, M., Hyun, Y., Lee, H., Choe, S., Kim, S.G., Michaels, S., and Lee, I. (2005). *SUPPRESSOR OF FRIGIDA3* encodes a nuclear ACTIN-RELATED PROTEIN6 required for floral repression in *Arabidopsis.* Plant Cell **17:** 2647–2660.

Choi, K., Park, C., Lee, J., Oh, M., Noh, B., and Lee, I. (2007). *Arabidopsis* homologs of components of the SWR1 complex regulate flowering and plant development. Development **134:** 1931–1941.

Clough, S.J., and Bent, A.F. (1998). Floral dip: A simplified method for *Agrobacterium*-mediated transformation of *Arabidopsis thaliana.* Plant J. **16:** 735–743.

Curtis, M.D., and Grossniklaus, U. (2003). A gateway cloning vector set for high-throughput functional analysis of genes *in planta.* Plant Physiol. **133:** 462–469.

Deal, R.B., Kandasamy, M.K., McKinney, E.C., and Meagher, R.B. (2005). The nuclear actin-related protein ARP6 is a pleiotropic developmental regulator required for the maintenance of *FLOWERING LOCUS C* expression and repression of flowering in *Arabidopsis.* Plant Cell **17:** 2633–2646.

Deal, R.B., Topp, C.N., McKinney, E.C., and Meagher, R.B. (2007). Repression of flowering in *Arabidopsis* requires activation of FLOWERING LOCUS C expression by the histone variant H2A.Z. Plant Cell **19:** 74–83.

Dou, Y., Milne, T.A., Ruthenburg, A.J., Lee, S., Lee, J.W., Verdine, G.L., Allis, C.D., and Roeder, R.G. (2006). Regulation of MLL1 H3K4 methyltransferase activity by its core components. Nat. Struct. Mol. Biol. **13:** 713–719.

Gazzani, S., Gendall, A.R., Lister, C., and Dean, C. (2003). Analysis of the molecular basis of flowering time variation in *Arabidopsis* accessions. Plant Physiol. **132:** 1107–1114.

Gu, X., Jiang, D., Wang, Y., Bachmair, A., and He, Y. (2009). Repression of the floral transition via histone H2B monoubiquitination. Plant J. **57:** 522–533.

He, Y., Doyle, M.R., and Amasino, R.M. (2004). PAF1-complex-mediated histone methylation of *FLOWERING LOCUS C* chromatin is required for the vernalization-responsive, winter-annual habit in *Arabidopsis.* Genes Dev. **18:** 2774–2784.

He, Y., Michaels, S.D., and Amasino, R.M. (2003). Regulation of flowering time by histone acetylation in *Arabidopsis.* Science **302:** 1751–1754.

He, Y. (2009). Control of the transition to flowering by chromatin modifications. Mol. Plant **2:** http://dx.doi.org/10.1093/mp/ssp1005.

Hilson, P., Allemeersch, J., Altmann, T., Aubourg, S., Avon, A., Beynon, J., Bhalerao, R.P., Bitton, F., Caboche, M., Cannoot, B., Chardakov, V., and Cognet-Holliger, C. (2004). Versatile gene-specific sequence tags for *Arabidopsis* functional genomics: Transcript profiling and reverse genetics applications. Genome Res. **14:** 2176–2189.

Jiang, D., Yang, W., He, Y., and Amasino, R.M. (2007). *Arabidopsis* relatives of the human Lysine-Specific Demethylase 1 repress the expression of *FWA* and *FLOWERING LOCUS C* and thus promote the floral transition. Plant Cell **19:** 2975–2987.

Jiang, D., Wang, Y., Wang, Y., and He, Y. (2008). Repression of *FLOWERING LOCUS C* and *FLOWERING LOCUS T* by the *Arabidopsis* Polycomb repressive complex 2 components. PLoS ONE **3:** e3404.

Johanson, U., West, J., Lister, C., Michaels, S., Amasino, R., and Dean, C. (2000). Molecular analysis of *FRIGIDA*, a major determinant of natural variation in *Arabidopsis* flowering time. Science **290:** 344–347.

Johnson, L., Cao, X., and Jacobsen, S. (2002). Interplay between two epigenetic marks. DNA methylation and histone H3 lysine 9 methylation. Curr. Biol. **12:** 1360–1367.

Karimi, M., De Meyer, B., and Hilson, P. (2005). Modular cloning in plant cells. Trends Plant Sci. **10:** 103–105.

Kim, S., Choi, K., Park, C., Hwang, H.J., and Lee, I. (2006). *SUPPRESSOR OF FRIGIDA 4*, encoding a C2H2-type zinc finger protein, represses flowering by transcriptional activation of *Arabidopsis FLOWERING LOCUS C.* Plant Cell **18:** 2985–2998.

Kim, S.Y., He, Y., Jacob, Y., Noh, Y.S., Michaels, S., and Amasino, R. (2005). Establishment of the vernalization-responsive, winter-annual habit in *Arabidopsis* requires a putative histone H3 methyl transferase. Plant Cell **17:** 3301–3310.

Kim, S.Y., and Michaels, S.D. (2006). *SUPPRESSOR OF FRI 4* encodes a nuclear-localized protein that is required for delayed flowering in winter-annual *Arabidopsis.* Development **133:** 4699–4707.

Lee, I., Michaels, S.D., Masshardt, A.S., and Amasino, R.M. (1994). The late-flowering phenotype of *FRIGIDA* and *LUMINIDEPENDENS* is suppressed in the Landsberg *erecta* strain of *Arabidopsis.* Plant J. **6:** 903–909.

Lee, M.G., Wynder, C., Bochar, D.A., Hakimi, M.A., Cooch, N., and Shiekhattar, R. (2006). Functional interplay between histone demethylase and deacetylase enzymes. Mol. Cell. Biol. **26:** 6395–6402.

Liu, F., Quesada, V., Crevillen, P., Baurle, I., Swiezewski, S., and Dean, C. (2007). The *Arabidopsis* RNA-binding protein FCA requires a Lysine-Specific Demethylase 1 homolog to downregulate *FLC.* Mol. Cell **28:** 398–407.

March-Diaz, R., Garcia-Dominguez, M., Florencio, F.J., and Reyes, J.C. (2007). SEF, a new protein required for flowering repression in *Arabidopsis*, interacts with PIE1 and ARP6. Plant Physiol. **143:** 893–901.

Martin-Trillo, M., Lazaro, A., Poethig, R.S., Gomez-Mena, C., Pineiro, M.A., Martinez-Zapater, J.M., and Jarillo, J.A. (2006). *EARLY IN SHORT DAYS 1* (*ESD1*) encodes ACTIN-RELATED PROTEIN 6 (AtARP6), a putative component of chromatin remodelling complexes that positively regulates *FLC* accumulation in *Arabidopsis.* Development **133:** 1241–1252.

Michaels, S., and Amasino, R. (1999). *FLOWERING LOCUS C* encodes a novel MADS domain protein that acts as a repressor of flowering. Plant Cell **11:** 949–956.

Michaels, S.D., Bezerra, I.C., and Amasino, R.M. (2004). *FRIGIDA*-related genes are required for the winter-annual habit in *Arabidopsis.* Proc. Natl. Acad. Sci. USA **101:** 3281–3285.

Michaels, S.D., He, Y., Scortecci, K.C., and Amasino, R.M. (2003). Attenuation of FLOWERING LOCUS C activity as a mechanism for the evolution of summer-annual flowering behavior in *Arabidopsis.* Proc. Natl. Acad. Sci. USA **100:** 10102–10107.

Miller, T., Krogan, N.J., Dover, J., Erdjument-Bromage, H., Tempst, P., Johnston, M., Greenblatt, J.F., and Shilatifard, A. (2001). COMPASS: A complex of proteins associated with a trithorax-related SET domain protein. Proc. Natl. Acad. Sci. USA **98:** 12902–12907.

Niu, L., Lu, F., Pei, Y., Liu, C., and Cao, X. (2007). Regulation of flowering time by the protein arginine methyltransferase AtPRMT10. EMBO Rep. **8:** 1190–1195.

Noh, Y.S., and Amasino, R.M. (2003). *PIE1*, an *ISWI* family gene, is required for *FLC* activation and floral repression in *Arabidopsis.* Plant Cell **15:** 1671–1682.

Oh, S., Zhang, H., Ludwig, P., and van Nocker, S. (2004). A mechanism related to the yeast transcriptional regulator Paf1c is required

for expression of the *Arabidopsis FLC/MAF* MADS box gene family. Plant Cell **16:** 2940–2953.

Pei, Y., Niu, L., Lu, F., Liu, C., Zhai, J., Kong, X., and Cao, X. (2007). Mutations in the Type II protein arginine methyltransferase AtPRMT5 result in pleiotropic developmental defects in *Arabidopsis.* Plant Physiol. **144:** 1913–1923.

Pien, S., Fleury, D., Mylne, J.S., Crevillen, P., Inze, D., Avramova, Z., Dean, C., and Grossniklaus, U. (2008). *ARABIDOPSIS* TRITHORAX 1 dynamically regulates *FLOWERING LOCUS C* activation via histone H3 lysine-4 trimethylation. Plant Cell **20:** 580–588.

Ratcliffe, O.J., Kumimoto, R.W., Wong, B.J., and Riechmann, J.L. (2003). Analysis of the *Arabidopsis MADS AFFECTING FLOWERING* gene family: *MAF2* prevents vernalization by short periods of cold. Plant Cell **15:** 1159–1169.

Rubio, V., Shen, Y., Saijo, Y., Liu, Y., Gusmaroli, G., Dinesh-Kumar, S.P., and Deng, X.W. (2005). An alternative tandem affinity purification strategy applied to *Arabidopsis* protein complex isolation. Plant J. **41:** 767–778.

Ruthenburg, A.J., Allis, C.D., and Wysocka, J. (2007). Methylation of lysine 4 on histone H3: intricacy of writing and reading a single epigenetic mark. Mol. Cell **25:** 15–30.

Ruthenburg, A.J., Wang, W., Graybosch, D.M., Li, H., Allis, C.D., Patel, D.J., and Verdine, G.L. (2006). Histone H3 recognition and presentation by the WDR5 module of the MLL1 complex. Nat. Struct. Mol. Biol. **13:** 704–712.

Saleh, A., Alvarez-Venegas, R., and Avramova, Z. (2008a). Dynamic and stable histone H3 methylation patterns at the *Arabidopsis FLC* and *AP1* loci. Gene **423:** 43–47.

Saleh, A., Alvarez-Venegas, R., Yilmaz, M., Le, O., Hou, G., Sadder, M., Al-Abdallat, A., Xia, Y., Lu, G., Ladunga, I., and Avramova, Z. (2008b). The highly similar *Arabidopsis* homologs of *TRITHORAX ATX1* and *ATX2* encode proteins with divergent biochemical functions. Plant Cell **20:** 568–579.

Samson, F., Brunaud, V., Balzergue, S., Dubreucq, B., Lepiniec, L., Pelletier, G., Caboche, M., and Lecharny, A. (2002). FLAGdb/FST: A database of mapped flanking insertion sites (FSTs) of *Arabidopsis thaliana* T-DNA transformants. Nucleic Acids Res. **30:** 94–97.

Schmitz, R.J., Hong, L., Michaels, S., and Amasino, R.M. (2005). *FRIGIDA-ESSENTIAL 1* interacts genetically with *FRIGIDA* and *FRIGIDA-LIKE 1* to promote the winter-annual habit of *Arabidopsis thaliana.* Development **132:** 5471–5478.

Schubert, D., Primavesi, L., Bishopp, A., Roberts, G., Doonan, J., Jenuwein, T., and Goodrich, J. (2006). Silencing by plant Polycomb-group genes requires dispersed trimethylation of histone H3 at lysine 27. EMBO J. **25:** 4638–4649.

Scortecci, K.C., Michaels, S.D., and Amasino, R.M. (2001). Identification of a MADS-box gene, *FLOWERING LOCUS M*, that represses flowering. Plant J. **26:** 229–236.

Sheldon, C.C., Burn, J.E., Perez, P.P., Metzger, J., Edwards, J.A., Peacock, W.J., and Dennis, E.S. (1999). The *FLF* MADS box gene: a repressor of flowering in *Arabidopsis* regulated by vernalization and methylation. Plant Cell **11:** 445–458.

Shi, Y., Lan, F., Matson, C., Mulligan, P., Whetstine, J.R., Cole, P.A., Casero, R.A., and Shi, Y. (2004). Histone demethylation mediated by the nuclear amine oxidase homolog LSD1. Cell **119:** 941–953.

Shilatifard, A. (2008). Molecular implementation and physiological roles for histone H3 lysine 4 (H3K4) methylation. Curr. Opin. Cell Biol. **20:** 341–348.

Spedaletti, V., Polticelli, F., Capodaglio, V., Schinina, M.E., Stano, P., Federico, R., and Tavladoraki, P. (2008). Characterization of a lysine-specific histone demethylase from *Arabidopsis thaliana.* Biochemistry **47:** 4936–4947.

Springer, N.M., Napoli, C.A., Selinger, D.A., Pandey, R., Cone, K.C., Chandler, V.L., Kaeppler, H.F., and Kaeppler, S.M. (2003). Comparative analysis of SET domain proteins in maize and *Arabidopsis* reveals multiple duplications preceding the divergence of monocots and dicots. Plant Physiol. **132:** 907–925.

Sung, S., and Amasino, R.M. (2005). Remembering winter: Toward a molecular understanding of vernalization. Annu. Rev. Plant Biol. **56:** 491–508.

Wang, X., Zhang, Y., Ma, Q., Zhang, Z., Xue, Y., Bao, S., and Chong, K. (2007). SKB1-mediated symmetric dimethylation of histone H4R3 controls flowering time in *Arabidopsis.* EMBO J. **26:** 1934–1941.

Werner, J.D., Borevitz, J.O., Uhlenhaut, N.H., Ecker, J.R., Chory, J., and Weigel, D. (2005). *FRIGIDA*-independent variation in flowering time of natural *Arabidopsis thaliana* accessions. Genetics **170:** 1197–1207.

Wysocka, J., Swigut, T., Milne, T.A., Dou, Y., Zhang, X., Burlingame, A.L., Roeder, R.G., Brivanlou, A.H., and Allis, C.D. (2005). WDR5 associates with histone H3 methylated at K4 and is essential for H3 K4 methylation and vertebrate development. Cell **121:** 859–872.

Zhao, Z., Yu, Y., Meyer, D., Wu, C., and Shen, W.H. (2005). Prevention of early flowering by expression of *FLOWERING LOCUS C* requires methylation of histone H3 K36. Nat. Cell Biol. **7:** 1256–1260.